

Observation and theoretical description of the pure Fano-effect in the valence-band photo-emission of ferromagnets

J. Minár and H. Ebert

*Department Chemie, Physikalische Chemie, Universität München,
Butenandtstr. 5-13, D-81377 München, Germany*

C. De Nadaï, N. B. Brookes and F. Venturini

*European Synchrotron Radiation Facility,
Boîte Postale 220, 38043 Grenoble Cedex, France*

G. Ghiringhelli

*INFM- Dip. di Fisica, Politecnico di Milano,
p. Leonardo da Vinci 32, 20133 Milano, Italy*

L. Chioncel* and M. I. Katsnelson

University of Nijmegen, NL-6525 ED Nijmegen, The Netherlands

**Institut für Theoretische Physik - Computational Physics,
Technische Universität Graz, A-8010 Graz, Austria*

A. I. Lichtenstein

Institut für Theoretische Physik, Universität Hamburg, 20355 Hamburg, Germany

(Dated: November 8, 2018)

Abstract

The pure Fano-effect in angle-integrated valence-band photo-emission of ferromagnets has been observed for the first time. A contribution of the intrinsic spin polarization to the spin polarization of the photo-electrons has been avoided by an appropriate choice of the experimental parameters. The theoretical description of the resulting spectra reveals a complete analogy to the Fano-effect observed before for paramagnetic transition metals. While the theoretical photo-current and spin difference spectra are found in good quantitative agreement with experiment in the case of Fe and Co only a qualitative agreement could be achieved in the case of Ni by calculations on the basis of plain local spin density approximation (LSDA). Agreement with experimental data could be improved in this case in a very substantial way by a treatment of correlation effects on the basis of dynamical mean field theory (DMFT).

Spin-resolved photo-emission spectroscopy is a powerful tool to study the magnetic aspects of the electronic structure of ferromagnetic materials. This could be demonstrated already about 25 years ago by the pioneering work of Eib and Alvarado[1] who investigated for Ni(110) the spin polarization of the photo-electrons in a photo-threshold experiment. More detailed information is obtained from spin-, energy- and angle-resolved photo-emission experiments that became feasible by the use of samples with a remanent magnetization oriented perpendicular to the electron-optical axis.[2] This technique was in particular used to study the dependence of the electronic and magnetic properties of the 3d-ferromagnets on temperature.[3] Even more refined experiments became possible by the use of circularly polarized radiation, that allows to study magnetic circular dichroism. As it could be demonstrated theoretically[4, 5] and experimentally,[6] spin-resolved photo-emission experiments using circularly polarized radiation allow in particular to reveal the hybridisation of states with different spin character due to spin-orbit coupling.

Magnetic circular dichroism in magnetically ordered systems is closely related to the Fano-effect[7] that also occurs as a consequence of the spin-orbit coupling. The term Fano-effect denotes the observation that one can have a spin-polarized photo-current from a non-magnetic sample if circularly polarized radiation is used for excitation. While for a non-magnetic sample the spin-polarization of the photo-current is reversed if the helicity of the radiation is reversed, this symmetry is in general broken for a magnetically ordered system leading to magnetic circular dichroism. This implies in particular that if a spin-resolved photo-emission experiment is done with circularly polarized radiation coming in along the direction of the magnetization of a ferromagnetic material and spin analysis of the photo-current is done with respect to this direction, the spin-polarization of the photo-current due to spin-orbit coupling is superimposed to that due to magnetic ordering. In the following it is demonstrated by experiments on Fe, Co and Ni that the pure Fano-effect can also be observed in angle-integrated valence band X-ray photo-emission spectroscopy (VB-XPS) for ferromagnets, if the circularly polarized radiation impinges perpendicular to the magnetization and if subsequent spin analysis is done with respect to the direction of the photon beam.

Accompanying calculations based on local spin-density approximation (LSDA) and using a fully relativistic implementation of the one-step model of photo-emission allow for a detailed discussion of the experimental spectra. As found before by comparable VB-XPS

investigations, calculations based on plain LSDA lead for Ni to a band width that seems to be too large compared with experiment and are not able to reproduce the satellite structure observed at 6 eV binding energy.[8, 9] These short comings have been ascribed to an inadequate treatment of correlation effects within LSDA. To remove these problems several approaches have been used in the past.[10, 11, 12, 13] Here we show that the use of LSDA in combination with dynamical mean field theory (DMFT) leads for Ni to a substantial improvement of the agreement of theoretical and experimental VB-XPS spectra.

The experiments were performed on the helical undulator beamline ID08 at the ESRF (European Synchrotron Radiation Facility). The APPLE II insertion device provides approximately 100% polarised soft X-rays (vertical and horizontal linearly polarised and left and right circularly polarised). All experiments have been performed on thin films (2–4 nm) prepared in-situ by e-beam growth on a clean Cu(001) substrate. The base pressure in the chamber was in the 10^{-11} mbar range. In all cases the shape anisotropy gave rise to an orientation of the magnetisation in-plane with a multidomain structure. The magnetisation of the sample was measured in remanence using X-ray magnetic circular dichroism. In the measuring geometry of normal incidence a vanishing dichroism signal was observed. The spin polarised photoemission measurements were performed at room temperature with the X-rays normal to the sample and the electrons were analysed with a hemispherical electron energy analyser with a $\pm 20^\circ$ angular acceptance at 60° to the incident light. Together with the polycrystalline nature of the samples this means that the measurement is angle integrated. The combined energy resolution was $\approx 0.5 - 0.7$ eV. The spin of the electrons was measured using a mini-Mott spin detector after the energy analysis [14]. In order to eliminate instrumental asymmetries the spectra were measured with both helicities of circular polarised light. This allows one to extract a spectra that is equivalent to the calculated spectra with a single helicity. The experimental spin polarisation is also corrected for the measuring geometry to give the spin polarisation along the light propagation direction.

To deal with the geometry of the photo-emission experiment described above we adopt the spin-density matrix formalism as described for example by Ackermann and Feder[15] for the angle-integrated case. This approach allows to express the photo-current and its spin polarization in terms of the spin density matrix

$$\rho(E') = \sum_{m_s m_{s'}} |m_s\rangle \tilde{I}_{m_s m_{s'}} \langle m_{s'}|, \quad (1)$$

with the angle-integrated spin dependent intensity function

$$\tilde{I}_{m_s m_{s'}}^{\lambda} = -\frac{1}{\pi} \Im \int d\hat{k} \langle \Psi_{m_s \vec{k}}^{final}(E') | X_{\vec{q}\lambda} G(E) X_{\vec{q}\lambda}^{\dagger} | \Psi_{m'_s \vec{k}}^{final}(E') \rangle . \quad (2)$$

Here the initial valence band states at energy E are represented by the single particle Green's functions $G(E)$ and absorption of radiation with wave vector \vec{q} , frequency ω and polarization λ represented by the electron-photon interaction operator $X_{\vec{q}\lambda}$ [16] is considered. The final states at energy $E' = E + \hbar\omega$ are given by a time-reversed spin-polarized LEED state.[15] With the spin density matrix ρ available the spin-averaged photo-current intensity \bar{I} and photo-electron spin polarization \vec{P} are given as $\bar{I} = \text{Trace } \rho$ and $\vec{P} = \text{Trace}(\vec{\sigma}\rho)/\bar{I}$, respectively, with $\vec{\sigma}$ the vector of spin matrices. Finally, if a spin analysis of the photo-current is performed with respect to a direction \hat{n} , the corresponding spin-projected photo-current I_{σ} is given by:

$$I_{\sigma}^{\lambda} = (1 + \sigma \vec{P} \cdot \hat{n}) \bar{I} / 2 \quad (3)$$

with $\sigma = \pm 1$ corresponding to spin-up and spin-down. In the following, the spin density matrix is defined with respect to a right-handed coordinate system with its z-axis chosen along the magnetization of the sample that in turn is oriented parallel to the surface plane. The x-axis coincides with the surface normal that specifies the direction \hat{n} for the spin analysis. To calculate the angle integrated spin-dependent intensity function $\tilde{I}_{m_s m_{s'}}$ given by Eq. (2) for a photo-emission experiment using circularly polarized radiation an appropriate extension of the fully relativistic approach worked out by Ebert and Schwitalla[17] has been made. This implies first of all that electronic properties are obtained within the framework of LSDA. To calculate the initial state Green's function and also the involved final states multiple scattering theory is used.[18] Because of the relatively high photon energy used in the experiments described below, the single-scatterer approximation has been used for the later ones. Finally, to compare theoretical spectra based on Eq. (3) various broadening mechanisms are incorporated in a phenomenological way. Intrinsic life-time effects are described by a Lorentzian-broadening with an energy dependent width $\Gamma(E) = a + b(E - E_F)^2$ with E_F the Fermi energy. Instrumental broadening in turn is accounted by Gaussian broadening with a broadening parameter σ . (For the spectra to be shown below the following parameters have been used: $a = 0.01$ eV, $b = 0.01$ eV $^{-1}$, $\sigma = 0.4$ eV).

When dealing with the Fano-effect in paramagnetic noble metals[19, 20] and in the ferromagnets Fe and Co (see below), the approach sketched above lead to theoretical spectra in rather good agreement with experiment. In the case of Ni, however, pronounced deviations occur that have to be ascribed to correlation effects that are not accounted for in an adequate way by LSDA. To remove these problems, we applied a recently proposed self-consistent KKR+DMFT scheme.[22] Within the relativistic extension of this approach, correlation effects are represented by a complex and local self-energy $\Sigma(E)$ that enters the Dirac-Hamiltonian used to calculate the Green's function $G(E)$ in Eq. (2). To calculate in turn $\Sigma(E)$, the most general rotationally invariant form of the generalized Hubbard (on-site) Hamiltonian[23] has been taken for the interaction Hamiltonian. Within DMFT, the many-body problem for a crystal is split into a one-particle impurity problem for the crystal and a many-body problem for one site in an effective medium (for the effective impurity method see for example Refs. 21, 24). The correlation effects are treated in the framework of dynamical mean field theory (DMFT) [21], with a spin-polarized T-matrix Fluctuation Exchange (SPTF) type of DMFT solver [25]. The SPTF approximation is a multiband spin-polarized generalization of the fluctuation exchange approximation (FLEX) [24, 26]. Since some part of the correlation effects are included already in the local spin-density approximation (LSDA) “double counted” terms should be taken into account. To this aim, we start with the LSDA electronic structure and replace $\Sigma_\sigma(E)$ by $\Sigma_\sigma(E) - \Sigma_\sigma(0)$ in all equations of the LSDA+DMFT method [27], the energy E being relative to the Fermi energy and $E_F = 0$. It means that we only add *dynamical* correlation effects to the LSDA method.

The experimental VB-XPS spectra of Fe, Co- and Ni recorded for a photon-energy of 600 eV and normalized to a peak height of 100 are shown on the left side in Fig. 1. No subtraction of the secondary background has been made. Comparison of the spectra with those of previous experimental work leads to a fairly good agreement. The right hand side of Fig. 1 gives the same scale the observed spin difference of the photo-current ΔI^+ , i.e. the difference of the currents of photo-electrons with spin-up and spin-down, for an excitation with left circularly polarized radiation. Because the polarisation analysis of the photo-current is done with respect to an axis that is perpendicular to the spontaneous magnetization \vec{m} , ΔI^+ cannot be caused by the exchange splitting of the ground state. In fact, one finds that the shape and amplitude of the ΔI^+ curves are very similar to that found for paramagnetic Cu.[19] This finding suggests that the observed spin difference

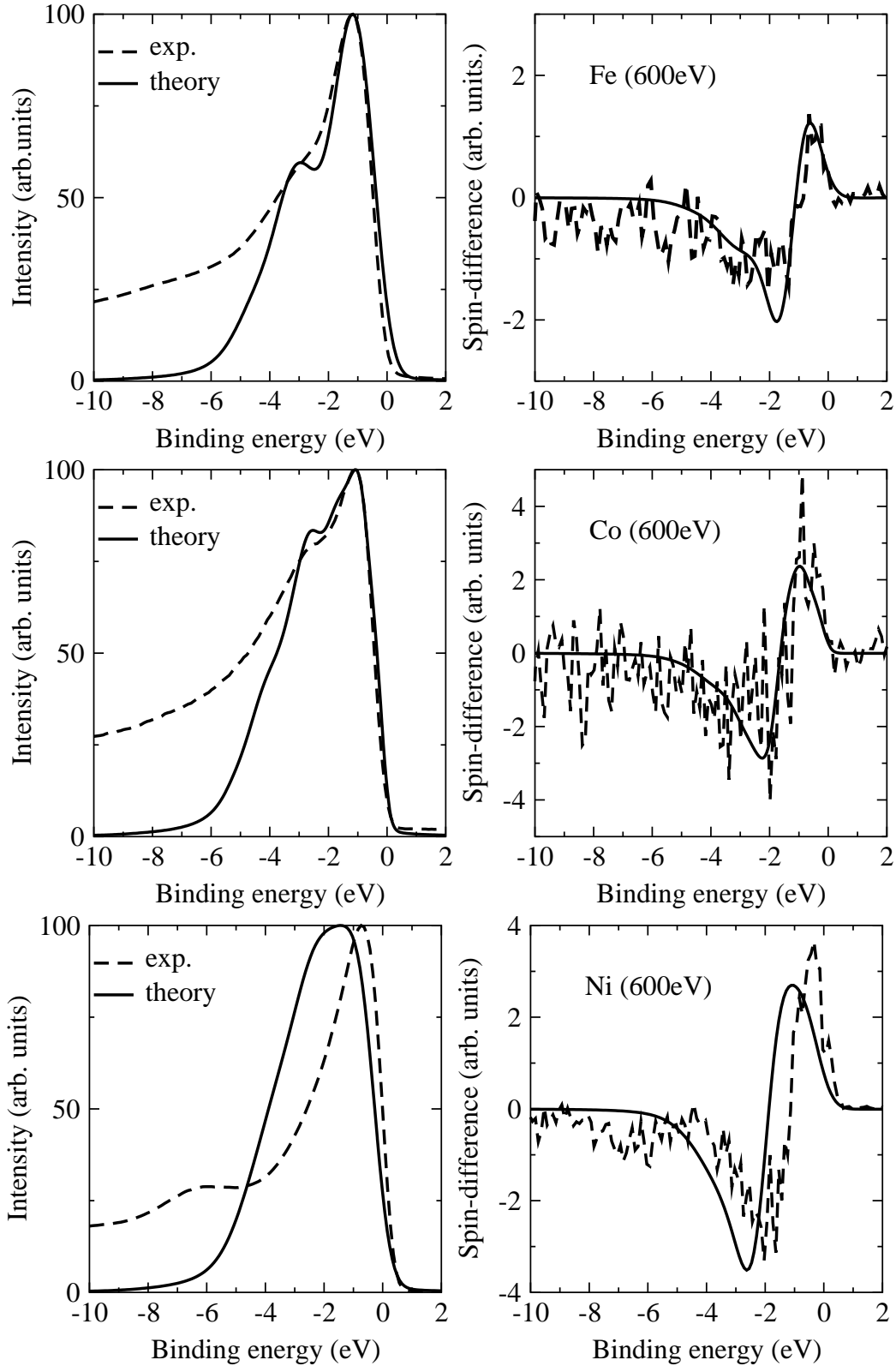


FIG. 1: Left: spin and angle-integrated VB-XPS-spectrum of ferromagnetic Fe, Co and Ni for a photon energy of 600 eV. Right: spin-difference $\Delta I^+ = I_\uparrow^+ - I_\downarrow^+$ of the photo-current for excitation with left circularly polarized radiation. Theory: full line; experiment: dashed line. The same scale has been used for the intensity and corresponding spin-difference plots.

reflects in both cases the Fano-effect that is due to the presence of spin-orbit coupling and the use of circularly polarized radiation for excitation. This can indeed be confirmed by an extension of the analytical model developed recently when dealing with the Fano-effect in the VB-XPS of paramagnetic solids.[19] To support this interpretation of the ΔI^+ spectra ab initio calculations have been performed along the lines sketched above. Taking into account the influence of the secondary electrons our theoretical results for the VB-XPS spectra are in fairly good agreement with experiment in the case of Fe and Co. For Ni, on the other hand, the LSDA-based calculations lead to a band-width that is much too large. Furthermore they are not able to reproduce the satellite at about 6 eV binding energy. To deal with this well-known problem connected with the valence-band photo-emission of Ni, additional calculations have been made on the basis of the LSDA+DMFT scheme (for the corresponding parameters see caption of Fig. 2). The resulting self-consistent complex and energy dependent self-energy $\Sigma(E)$ is shown in Fig. 2 in a spin- and symmetry-resolved way. The appreciable real part of $\Sigma(E)$ gives rise to a corresponding shrinking of the d-band

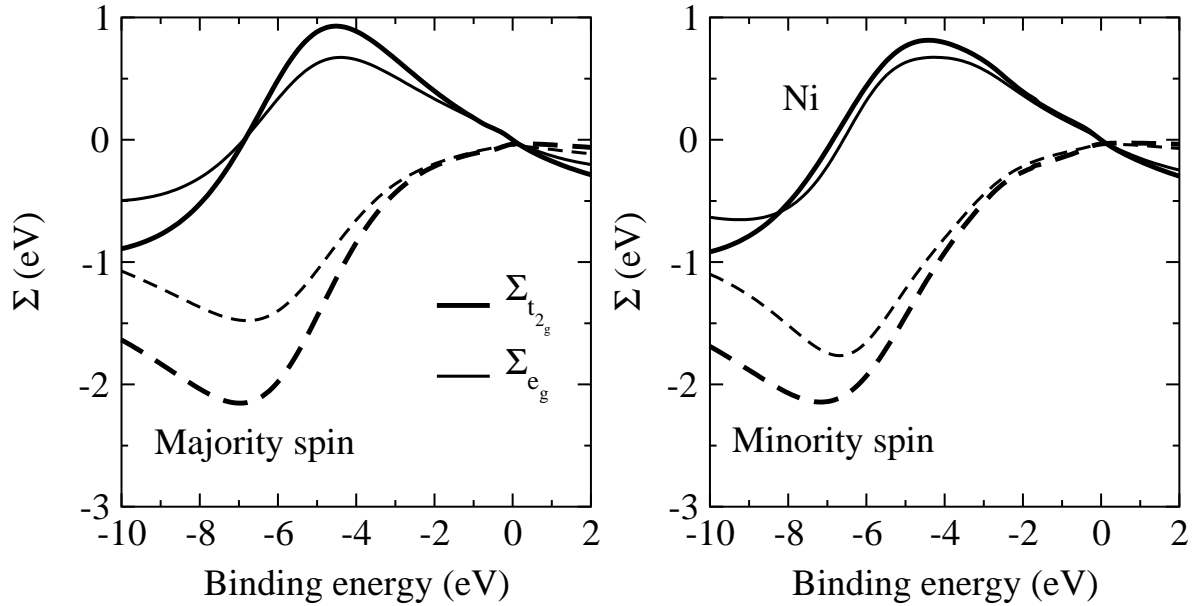


FIG. 2: The spin resolved self-energies of ferromagnetic Ni calculated within the DMFT for $U=3$ eV, $J=0.9$ eV and $T=500$ K. The real parts (full lines) and imaginary parts (dashed lines) are shown separately for the t_{2g} (thick lines) and e_g (thin lines) representations of the d-states.

width of Ni. This leads to a much better agreement of the theoretical VB-XPS spectrum

with experiment, as can be seen in Fig. 3. In addition, use of the LSDA+DMFT scheme

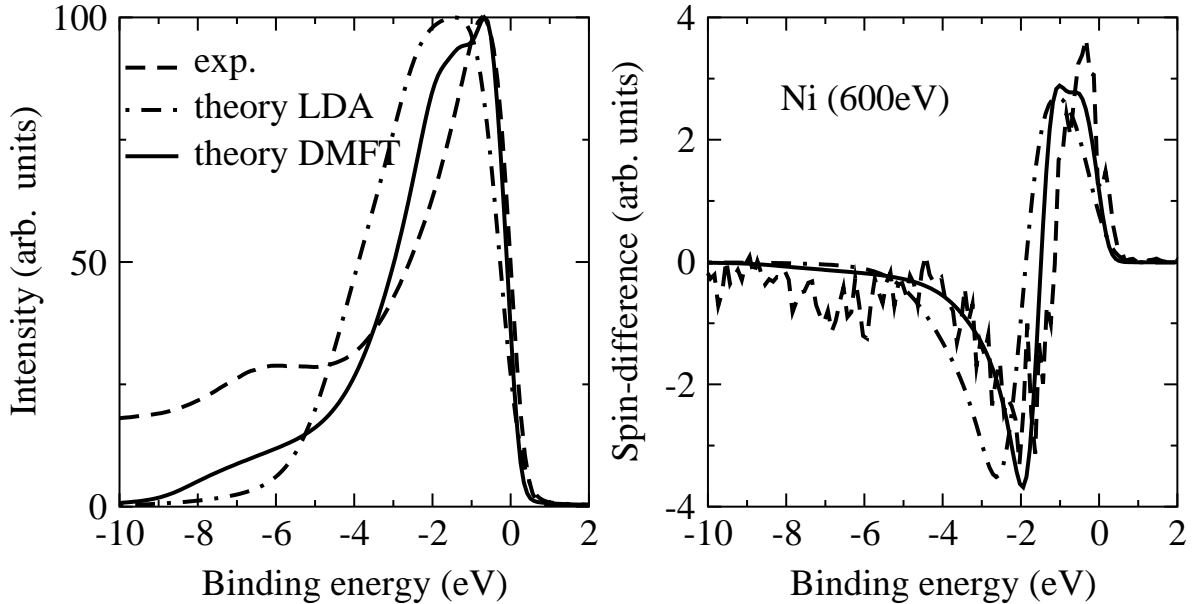


FIG. 3: Left: The experimental (dashed lines), theoretical LSDA (dot dashed lines) and LSDA+DMFT (full line) data for spin and angle integrated VB-XPS spectra of Ni for a photon energy of 600 eV. Right: spin-difference $\Delta I^+ = I_\uparrow^+ - I_\downarrow^+$ of the photo-current for excitation with left circularly polarized radiation.

leads to a pronounced increase of the intensity in the regime of the 6 eV satellite.

The theoretical spin difference ΔI^+ shown on the right hand side of Fig. 1 is found in rather good agreement with experiment in particular for Fe and Co. As mentioned, the shape and amplitude of the curves are very similar to that found for paramagnetic Cu. In fact, performing model calculations for Fe, Co and Ni with the exchange splitting suppressed, i.e. for a hypothetical paramagnetic state, one obtains ΔI^+ curves that differ not very much from those for the ferromagnetic state (in particular for Fe and Co the curves differ somewhat with respect to shape and amplitude). The sequence for the maximum (minimum) of ΔI^+ of Fe, Co and Ni is found to be 1.3, 2.2 and 2.6 (-1.9, -2.7 and -3.5). Although there are several electronic and structural properties that determine these data, they nevertheless correlate reasonably well with the strength of the spin-orbit coupling parameters of the d-states (66, 85 and 107 meV, respectively)[28] to identify once more the spin-orbit coupling as the source for the observed spin-polarization. Performing calculations for a reversed helicity λ of the

radiation leads to a reversed sign for the spin polarisation ΔI^λ . This is an additional proof that the pure Fano-effect is indeed observed by the experimental set-up described above. As for the standard VB-XPS spectra inclusion of the self-energy $\Sigma(E)$ leads to a substantial improvement for the agreement of the theoretical ΔI^+ spectrum with experiment. As one can see in Fig. 3 the shrinking of the band width is also reflected by the ΔI^+ curves, while their amplitude and shape is only slightly changed.

In conclusion, it has been demonstrated that the pure Fano-effect in angle-integrated VB-XPS can also be observed in ferromagnets if an appropriate geometry is chosen. The interpretation of the resulting spin polarization spectra can be done in complete analogy as for the paramagnetic case. Corresponding ab initio calculations allow in particular a quantitative description of the effect. Concerning this it could be demonstrated that an improved description of correlation effects on the basis of the LSDA+DMFT scheme leads to a substantially improved agreement of the theoretical and experimental spectra. This implies that achievements made for other systems by use of the DMFT can be monitored by our new combined approach in a most stringent way by comparing calculated photoemission spectra, that include all matrix element effects, directly to corresponding experimental data.

This work was funded by the German BMBF (Bundesministerium für Bildung und Forschung) under contract FKZ 05 KS1WMB/1.

- [1] W. Eib and S. F. Alvarado, Phys. Rev. Letters **37**, 444 (1976).
- [2] E. Kisker, W. Gudat, E. Kuhlmann, R. Clauberg, and M. Campagna, Phys. Rev. Letters **45**, 2053 (1980).
- [3] E. Kisker, K. Schröder, M. Campagna, and W. Gudat, Phys. Rev. Letters **52**, 2285 (1984).
- [4] T. Scheunemann, S. V. Halilov, J. Henk, and R. Feder, Solid State Commun. **91**, 487 (1994); J. Henk, M. Hoesch, J. Osterwalder, A. Ernst, and P. Bruno, J. Phys.: Cond. Matt. **16**, 7581 (2004).
- [5] J. Braun, Rep. Prog. Phys. **59**, 1267 (1996).
- [6] W. Kuch and C.-M. Schneider, Rep. Prog. Phys. **64**, 147 (2001).
- [7] U. Fano, Phys. Rev. **184**, 250 (1969).
- [8] S. Hüfner and G. K. Wertheim, Solid State Commun. **11**, 323 (1972).

- [9] S. Hüfner and G. K. Wertheim, Phys. Letters **51A**, 299 (1975).
- [10] A. Liebsch, Phys. Rev. Letters **43**, 1431 (1979).
- [11] F. Aryasetiawan, Phys. Rev. B **46**, 13051 (1992).
- [12] J. I. Igarashi, P. Unger, K. Hirai, and P. Fulde, Phys. Rev. B **49**, 16181 (1994).
- [13] F. Manghi, V. Bellini, J. Osterwalder, T. J. Kreutz, P. Aebi, and C. Arcangeli, Phys. Rev. B **59**, R10409 (1999).
- [14] G. Ghiringhelli, K. Larsson, and N. B. Brookes, Rev. Sci. Instrum. **70**, 4225 (1999).
- [15] B. Ackermann and R. Feder, Solid State Commun. **54**, 1077 (1985).
- [16] M. E. Rose, *Relativistic Electron Theory* (Wiley, New York, 1961).
- [17] H. Ebert and J. Schwitalla, Phys. Rev. B **55**, 3100 (1997).
- [18] H. Ebert, in *Electronic Structure and Physical Properties of Solids*, edited by H. Dreyssé (Springer, Berlin, 2000), vol. 535 of *Lecture Notes in Physics*, p. 191.
- [19] J. Minár, H. Ebert, G. Ghiringhelli, O. Tjernberg, N. B. Brookes, and L. H. Tjeng, Phys. Rev. B **63**, 144421 (2001).
- [20] C. De Nadai, J. Minár, H. Ebert, G. Ghiringhelli, A. Tagliaferri, and N. B. Brookes, Phys. Rev. B **70**, 134409 (2004).
- [21] A. Georges, G. Kotliar, W. Krauth, and M. J. Rozenberg, Rev. Mod. Phys. **68**, 13 (1996).
- [22] J. Minár, L. Chioncel, A. Perlov, H. Ebert, M. I. Katsnelson, and A. I. Lichtenstein, Phys. Rev. B **72**, 045125 (2005).
- [23] V. Anisimov, F. Aryasetiawan, and A. I. Lichtenstein, J. Phys.: Condensed Matter **9**, 767 (1997).
- [24] M. Katsnelson and A. Lichtenstein, Journal of Physics: Condensed Matter **11**, 1037 (1999).
- [25] M. I. Katsnelson and A. I. Lichtenstein, European Physics Journal B **30**, 9 (2002).
- [26] N. E. Bickers and D. J. Scalapino, Ann. Phys. (NY) **193**, 206 (1989).
- [27] A. I. Lichtenstein, M. I. Katsnelson and G. Kotliar, Phys. Rev. Letters **87**, 067205 (2001).
- [28] V. Popescu, H. Ebert, B. Nonas, and P. H. Dederichs, Phys. Rev. B **64**, 184407 (2001).